Eur J Vasc Endovasc Surg (2019) 58, 415–425

Dissection Level Within Aortic Wall Layers is Associated with Propagation of Type B Aortic Dissection: A Swine Model Study

Baolei Guo [a,†], **Zhihui Dong** [a,†], **Selene Pirola** [b,†], **Yifan Liu** [a], **Claudia Menichini** [b], **Xiao Yun Xu** [b], **Daqiao Guo** [a,**], **Weiguo Fu** [a,*]

[a] Department of Vascular Surgery, Zhongshan Hospital Fudan University, Shanghai, China
[b] Department of Chemical Engineering, Imperial College London, South Kensington Campus, London, UK

WHAT THIS PAPER ADDS

This *in vivo* study shows that deeper intimal tears, especially when the primary tear occurs on the adventitial side of the media, result in greater dissection propagation in a swine model of type B aortic dissection. This might have important consequences for clinicians to understand the complex pathology and haemodynamics of aortic dissection.

Objective: Haemodynamic and geometric factors play pivotal roles in the propagation of acute type B aortic dissection (TBAD). The aim of this study was to evaluate the association between dissection level within all aortic layers and the propagation of acute TBAD in porcine aorta.

Methods: In twelve pigs, two models of TBAD were created. In model A (n = 6), the aortic wall tear was superficial and close to the intima (thin intimal flap), whereas in model B (n = 6) it was deep and close to the adventitia (thick intimal flap). Dissection propagation was evaluated using angiography or computed tomography scans, and the haemodynamic measurements were acquired using Doppler wires. Most pigs were followed up at 1, 3, 6, 12, 18, and up to 24 months; four animals were euthanised at three and six months, respectively (two from each group).

Results: Both models were successfully created. No statistical difference was observed for the median antegrade propagation distance intra-operatively between the two models ($p = .092$). At 24 months, the longitudinal propagation distance was significantly greater in model B than in model A ($p = .016$). No statistical difference in retrograde propagation was noted ($p = .691$). Over time, aortic wall dissection progressed most notably over the first three months in model A, whereas it continued over the first 12 months in model B. Flow velocity was significantly greater in the true lumen than in false lumen at the level of the primary tear ($p = .001$) and in the middle of the dissection ($p = .004$). The histopathological images at three and six months demonstrated the fibres were stretched linearly at the outside wall of false lumen in both models, while the depth of intimal tears developed to be superficial and similar at the distal dissection.

Conclusion: In this swine model of TBAD, a deeper intimal tear resulted in greater dissection propagation.

Keywords: Intimal tear, Propagation, Swine model, Type B aortic dissection
Article history: Received 7 February 2018, Accepted 22 February 2019, Available online 20 July 2019

INTRODUCTION

Recent developments in endograft design and endovascular procedures for the treatment of type B aortic dissection (TBAD) have led to timely appraisals and improved understanding of the haemodynamics of dissection.[1] The pulsatile blood flow pressure within the aortic wall after dissection causes extension of the dissection. The dissection flap may be localised, or it may spiral along the entire length of the aorta. Arterial pressure and shear forces may lead to further tears in the intimal flap, producing secondary tears or re-entry tears that create blood flow communications between the true lumen (TL) and false lumen (FL). However, the propagation of a dissection is an acute phenomenon that is rarely observed clinically. At present, the biomechanical factors responsible for the initiation and propagation of TBAD are not fully understood.[2,3]

Model studies focusing on aortic morphology and dissection propagation may provide insights into the role of flap movement and primary and secondary entry tears for a

† Contributed equally to this work and share co-first authorship.
* Corresponding author. Department of Vascular Surgery, Zhongshan Hospital Fudan University; Institute of Vascular Surgery, Fudan University, 180# Fenglin Road, 200032, Shanghai, PR China.
** Corresponding author. Department of Vascular Surgery, Zhongshan Hospital Fudan University, Institute of Vascular Surgery, Fudan University, 180# Fenglin Road, 200032, Shanghai, PR China.
E-mail addresses: guo.daqiao@zs-hospital.sh.cn (Daqiao Guo); fu.weiguo@zs-hospital.sh.cn (Weiguo Fu).

https://doi.org/10.1016/j.ejvs.2019.02.026

better understanding of the pathology of TBAD. Recent work has concentrated on examining the haemodynamic forces in TBAD, primarily using computational fluid dynamics models,[4–6] finite element analysis,[7,8] or fluid structure interaction simulations of TBAD.[9,10] However, most of these simulations have been based on simplifying assumptions and non-patient specific boundary conditions, which can give rise to substantial bias and many limitations.

Regardless of the complexity of blood flow, vascular geometry and haemodynamics play pivotal roles in the initiation, acute propagation, and chronic development of TBADs.[11] Therefore, *in vivo* histological and haemodynamic studies of TBAD are the preferred methods for defining the underlying pathophysiological mechanisms. At present, few *in vivo* studies have provided direct observation of the pre- and post-propagation conditions of dissection. In this study, *in vivo* TBAD models were created to evaluate the association between dissection level within aortic wall layers and the propagation of acute TBAD in porcine aorta.

METHODS

The study was approved by the Institutional Animal Care and Use Committee of Fudan University. All surgical experiments and euthanasia were performed according to the principles of laboratory animal care advocated by the animal experiment committee of Zhongshan Hospital Fudan University. The animals were provided by the Laboratory Animal Centre of Gateway (Shanghai, China).

Animal care

Twelve Shanghai Landrace pigs (aged 7—10 months; seven males), weighing an average of 71.2 kg (range 67.4—72.5 kg), were used in the present study. Each animal was sedated with an intramuscular injection of ketamine hydrochloride (15 mg/kg) and atropine sulphate (0.04 mg/kg). General anaesthesia was induced with isoflurane (5%) administered with a face mask and a target controlled infusion (TCI) of remifentanil at 4 ng/mL. To facilitate endotracheal intubation, rocuronium was given at 0.5 mg/kg. After intubation, anaesthesia was maintained with isoflurane (1.5—3%), oxygen (0.8—1.5 L/minute) and mechanical ventilation. The TCI of remifentanil was reduced to match the level of surgical stimulation.

Creation of the TBAD model

After induction of general anaesthesia and prophylactic amoxicillin/clavulanate (antibiotic) administration, swine were placed in the supine position. Invasive blood pressure monitoring was established in the left femoral artery. Heparin (50 IU/kg) was administered intravenously, with additional doses as required to achieve an activated clotting time of >300 s. A stab incision was made in the right groin and an introducer sheath (7 Fr) was inserted via the right femoral artery. A 0.035 inch guidewire (Terumo, Tokyo, Japan) and a 4 Fr pigtail catheter were advanced into the thoracic and abdominal aorta to allow for full angiographic evaluation of the aorta and its branches.

All procedures were performed by two experienced operators. The descending aorta was approached via a left thoracotomy at the fifth to seventh intercostal space. The descending aorta was mobilised for 20—25 cm, from the ligamentum arteriosum to the distal end of the descending aorta. Two pairs of intercostal arteries in the operative area were ligated. Once there was haemodynamic stability, the descending aorta was completely cross clamped at both ends of the distally mobilised area. The descending aorta was then incised transversely along one-third to half of its circumference to create the entry tear. The dissecting aortic layers was made in the plane of media in the 12 o'clock position, first with a Freer elevator and then with Debakey forceps, which created an entry pocket extending to one quarter of the aortic circumference. In model A ($n = 6$), the primary tear was created on the intimal side of the media in the descending aorta (Fig. 1, A1). In model B ($n = 6$), the primary tear was created on the adventitial side of the media (Fig. 1, B1). The media was then mobilised approximately 1—2 cm distally to make the entry pocket. The adventitia and part of the media were then sutured with 6-0 Prolene continuous U shaped sutures, which resulted in the pathological basis of the aortic dissection. The anastomosis was reinforced with 7-0 Prolene interrupted sutures.

The distal clamp was removed to check for bleeding at the anastomosis. The proximal clamp was then loosened step by step and completely removed when the haemodynamics were stable. The creation of the dissection was then evaluated using angiography and the thoracotomy was closed in layers. A chest tube was inserted through a short cut in the skin beside the wound. The sheath in the femoral artery was removed and haemostasis was achieved by manual compression. The animals were extubated and returned to their cages.

Propagation observations and image examinations

All animals underwent post-procedural aortography. Technical success was defined as the successful creation of a dissection (FL length > 20 mm), as identified by the final angiogram. Propagation was defined as an increase in the size of a FL. The animals were maintained on a normal diet until follow up evaluation. Acetylsalicylic acid was administrated at a dosage of 100 mg daily. Follow up observations were performed by computed tomography angiography (CTA) at 1, 3, 6, 12, 18, and 24 months, in all animals that were not sacrificed.

Haemodynamic evaluation by Doppler wire

Haemodynamic evaluation of the TBAD models were performed one month post-procedure using Doppler wires. The intravascular Doppler device used was the ComboMap system (Volcano; San Diego, CA, USA) (Appendix S1; Supplementary Material).

Histological analysis

Some animals were euthanised at three months ($n = 2$, one from each group) and six months ($n = 2$, one of each group). For histological evaluation, the aorta of each pig

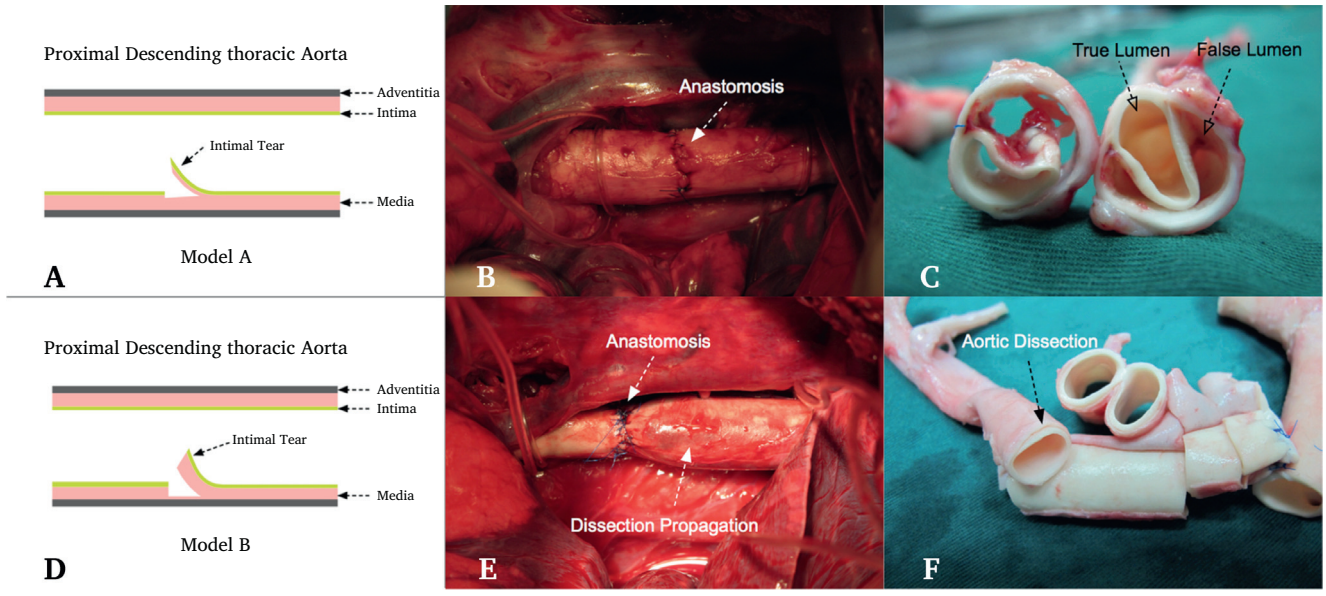

Figure 1. A schematic diagram of the two type B aortic dissection models (A - C for model A; D - F for model B). In both models, an intimal tear, which included the intima and parts of media, was made at the proximal descending thoracic aorta using a transverse incision. The proximal free edge of the aortic wall and the outer layer of the distal aortic wall were sutured with 6-0 Prolene with the animals under general anaesthesia (B and E). Macroscopic examination revealed that at three months the dissections showed different propagation and flap characteristics (C and F).

was carefully removed with its adipose tissue and fixed in 10% phosphate buffered formaldehyde. Cross sections (5 mm) of the vascular tissues were obtained and embedded in paraffin. Subsequently, serial sections of 3–5 µm thickness were cut at the level of proximal (2 cm below the proximal entry tear) and distal dissection (2 cm above the distal entry tear) and stained with resorcinol fuchsin to show the elastic fibres. These sections were examined by light microscopy by an experienced pathologist.

Statistical analysis

Data were assessed for normality and expressed as *n* (%) for categorical and median (range) for continuous variables. Continuous variables were compared using the Mann–Whitney *U* test for non-normal distribution data. Categorical variables were compared using the chi-square test or Fisher's exact test. The velocity between the TL and FL and the increase in aortic diameter over time between the two models were compared using the non-parametric Wilcoxon signed rank test for paired data. The study data were analysed using SPSS version 20.0 (IBM, Armonk, NY, USA). A p value < 0.05 was considered statistically significant.

RESULTS

TBAD model

Table 1 shows the average diameters of the aorta and branches in the 12 animals. The TBAD was successfully created and confirmed by angiography and/or CTA in all animals (Fig. 2). Intra-operative angiography revealed luminal flow with clear delineation of the septal flap. Median time for establishing the TBAD models was 45.1 min (range 30.6–53.6 min) and the duration of total aortic occlusion was 18.3 min (range 15.7–28.9 min). These variables did not differ statistically between the two models. The initial aortic diameter at the primary tear of the created dissection ranged from 13.9 to 24.1 mm. Intra-operative longitudinal propagation length was 39.0 mm (range 30.6–48.4 mm) in model A and 57.0 mm (range 47.4–65.4 mm) in model B ($p = .092$; Fig. 3A). The intra-operative maximum diameter of the aortic dissection was much larger in model B than model A ($p = .022$; Fig. 3B). On the first post-procedural day, two animals died, one due to anaesthesia related complications (in model A) and a second due

Table 1. Diameters of the aorta and peripheral arteries in the 12 study animals (Shanghai landrace pigs)

Variable	Median (range) - mm
Ascending aorta	25.4 (23.0–26.8)
Aortic arch	21.2 (18.6–26.6)
Innominate artery	11.0 (9.3–13.6)
Left subclavian artery	10.4 (8.5–11.9)
Proximal thoracic aorta	23.5 (17.9–26.9)
Middle thoracic aorta	19.6 (14.6–22.8)
Distal thoracic aorta	16.2 (12.6–18.6)
Coeliac trunk	6.2 (5.3–7.8)
Superior mesenteric artery	8.8 (7.2–9.4)
Renal artery	6.7 (5.6–8.3)
Proximal abdominal aorta	13.3 (12.3–18.4)
Middle abdominal aorta	12.2 (11.0–16.3)
Distal abdominal aorta	12.0 (10.4–15.9)
Iliac artery	7.8 (7.4–9.6)
Femoral artery	6.2 (5.9–6.9)

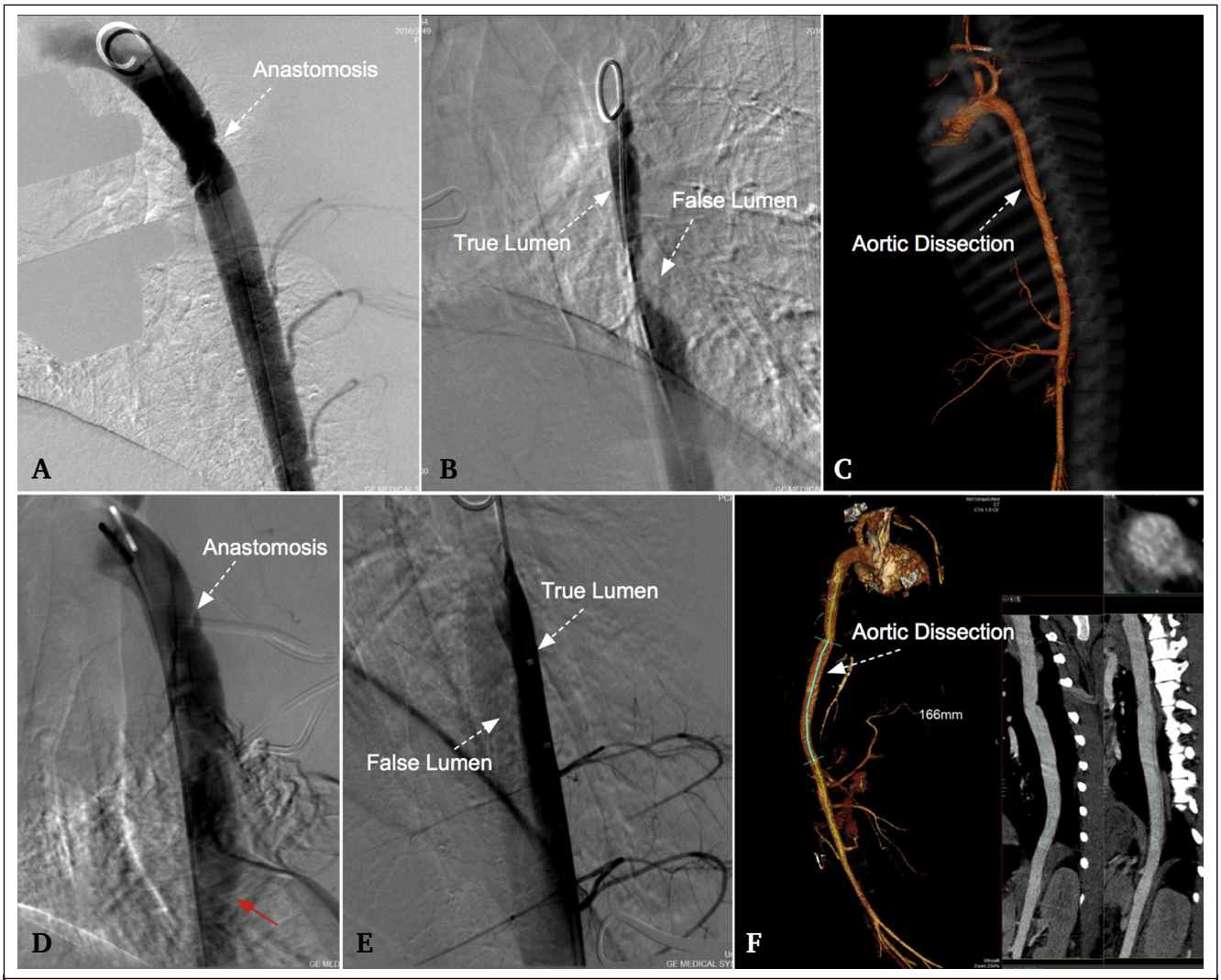

Figure 2. Dissection propagation during six months of follow up in the two models (A - C for model A; D - F for model B). Aortography immediately after creation of the dissections showed no dissection propagation in model A (A), whereas a significant longitudinal propagation occurred in model B (D, red arrow). In both models, the extension of the dissection in the thoraco-abdominal aorta was similar one month after the first procedure (B and E) to the imaging findings obtained with computed tomography angiography at six months (C and F).

to aortic rupture (in model B). One animal suffered an incision infection. No other complications occurred in the nine remaining animals.

Haemodynamics and dissection propagation

Over 30 days of follow up, haemodynamic measurements were successfully performed using the Doppler wire in seven of 10 animals. Three animals were excluded from haemodynamic analysis in the study, because the short FL and movement of dissection flap seriously influenced the quality of measurements in the FL. A stable, high quality Doppler wire signal was hard to obtain in a small FL during the cardiac cycle. Heart rate was maintained in a stable range (median 86 beats per minute [bpm]; range 78—95 bpm) under general anaesthesia. Average peak velocity was significantly higher in the TL than in the FL at the level of the primary tear ($p = .001$) and the middle of dissection ($p = .004$; Fig. 4). Dissection propagations of all animals were observed according to CTA findings at the 30 day follow up. There was a significant difference in median propagation length between the two groups (model A: 73.4 mm [range 51.9—95.0 mm]; model B: 161.2 mm [range 109.2—213.1 mm]; $p = .016$). During follow up, eight animals showed re-entry tears located at the ostium of the aortic branch vessels ($n = 8/10$ [80%]), including four tears at the intercostal artery, two at the coeliac trunk, and two at the superior mesenteric artery (Fig. 5). The antegrade propagation length at 24 months was significantly longer in model B (180.4 mm [range 127.5—251.6 mm]) compared with model A (81.8 mm [range 52.8—113.2 mm]; $p = .016$). The retrograde propagation length did not differ between the two models ($p = .691$). The total propagation length was observed for longer in model B than in model A during follow up ($p = .032$; Fig. 3). Notably, acute dissection propagation occurred at any time but was most common in the first three months in model A and in the first 12 months in model B. The maximum diameter of dissection in model A

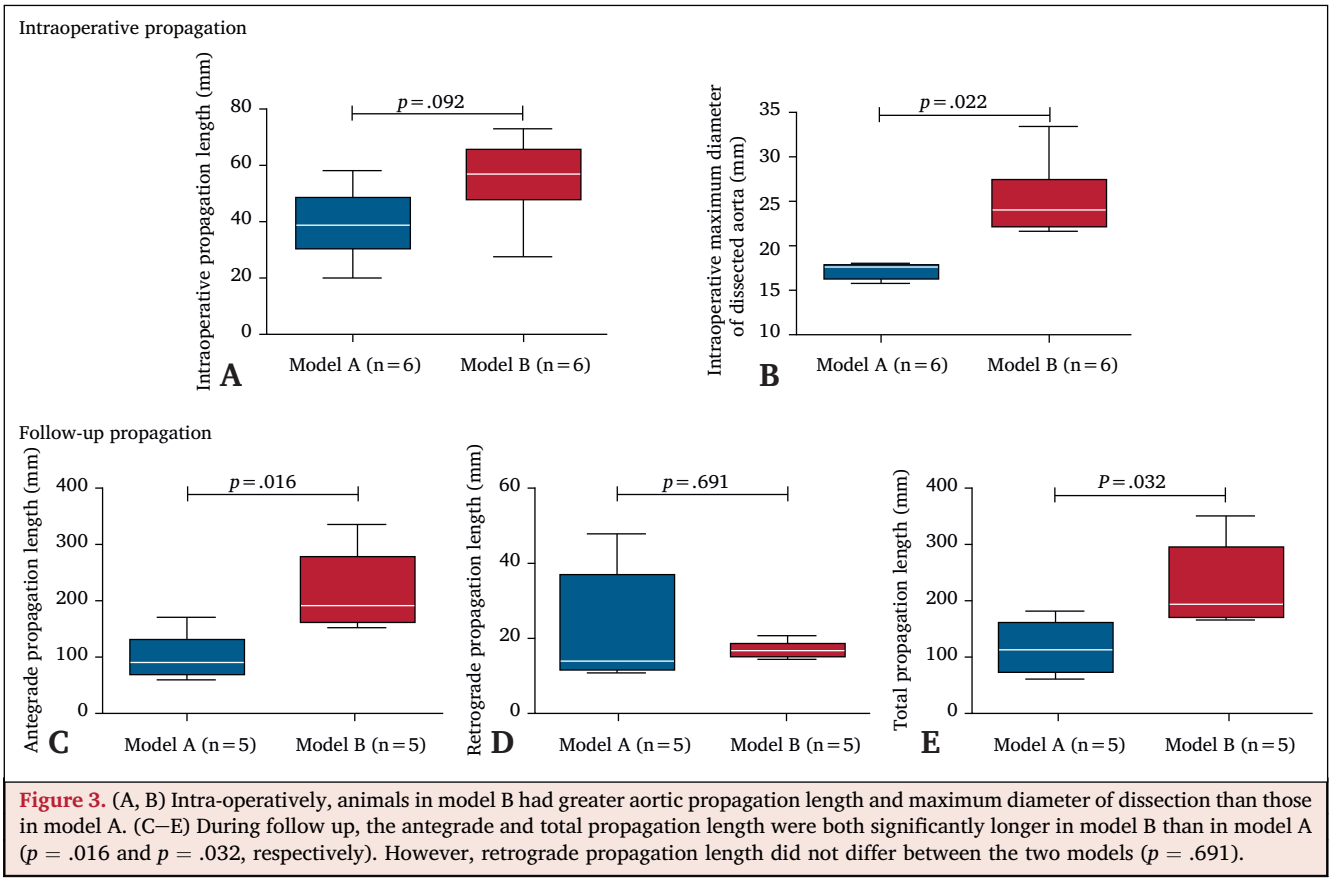

Figure 3. (A, B) Intra-operatively, animals in model B had greater aortic propagation length and maximum diameter of dissection than those in model A. (C–E) During follow up, the antegrade and total propagation length were both significantly longer in model B than in model A ($p = .016$ and $p = .032$, respectively). However, retrograde propagation length did not differ between the two models ($p = .691$).

at the 24 month follow up was seen to be larger than that at one month follow up ($p = .046$), whereas in model B it seemed only to increase after 12 months. However, no statistical difference in maximum diameter was observed in model B ($n = 3$) during the second year follow up (27.8 mm at 12 months vs. 33.8 mm at 24 months [$p = .11$]; Fig. 6). During follow up, there were no FL thromboses in either model, according to CTA.

Histological findings

Microscopy showed that the created dissection was located correctly in the different planes of the medial layer of the aorta. Histological findings of the two models were generally concordant with the macroscopic examination. Microscopy revealed that the dissecting plane was located deep within the inner media in model A, whereas this plane was much closer to the adventitia in model B (Fig. 7A). The different intimal tear locations were observed at the proximal dissection in both models; however, the intimal tears developed to be superficial and similar at the distal dissection (Fig. 7B and C). In both models, the shape and orientation of elastin and collagen fibres were different on both sides of the FL. The elastin and collagen were of a wavy arrangement inside the FL, whereas the fibres were in alignment on the outside of the FL. The fibres were much more stretched on the adventitia and outside the media than on the intima side.

DISCUSSION

Acute TBAD is the result of a tear in the intimal arterial layer, which allows blood to propagate within the medial layer. Generally, the created intimal flap divides the aorta into two channels, resulting in haemodynamic redistribution.[12,13] However, according to current guidelines, it is unclear whether the layers of dissecting flap impact on the propagation of TBAD.[13,14] The swine TBAD models in the present study demonstrated that a deeper intimal tear resulted in greater aortic dissection propagation. This finding may shed new light on the role of the dissecting flap in the evolvution of aortic propagation and dilatation.

Numerous unsatisfactory attempts have been made to simulate human aortic dissection in canines,[15–17] while only a few studies have been conducted with swine.[18,19] A previous study demonstrated that there seemed to be few structural differences between human and porcine thoracic aortic tissue.[20] In particular, in the ascending aorta, the stiffness of young porcine aortic tissue (0.5–12 months) corresponded well with human tissue $<$ 60 years. The *ex vivo* porcine aortic models reported by Qing et al. also proved to be useful and reproducible to study the complex haemodynamics of TBAD.[21] The present swine TBAD models are reproducible and resemble human models, but swine models do have some shortcomings, including anaesthesia tolerance and post-operative management.

In the models presented here, the findings suggest that the depth of the initial dissected flap significantly influences

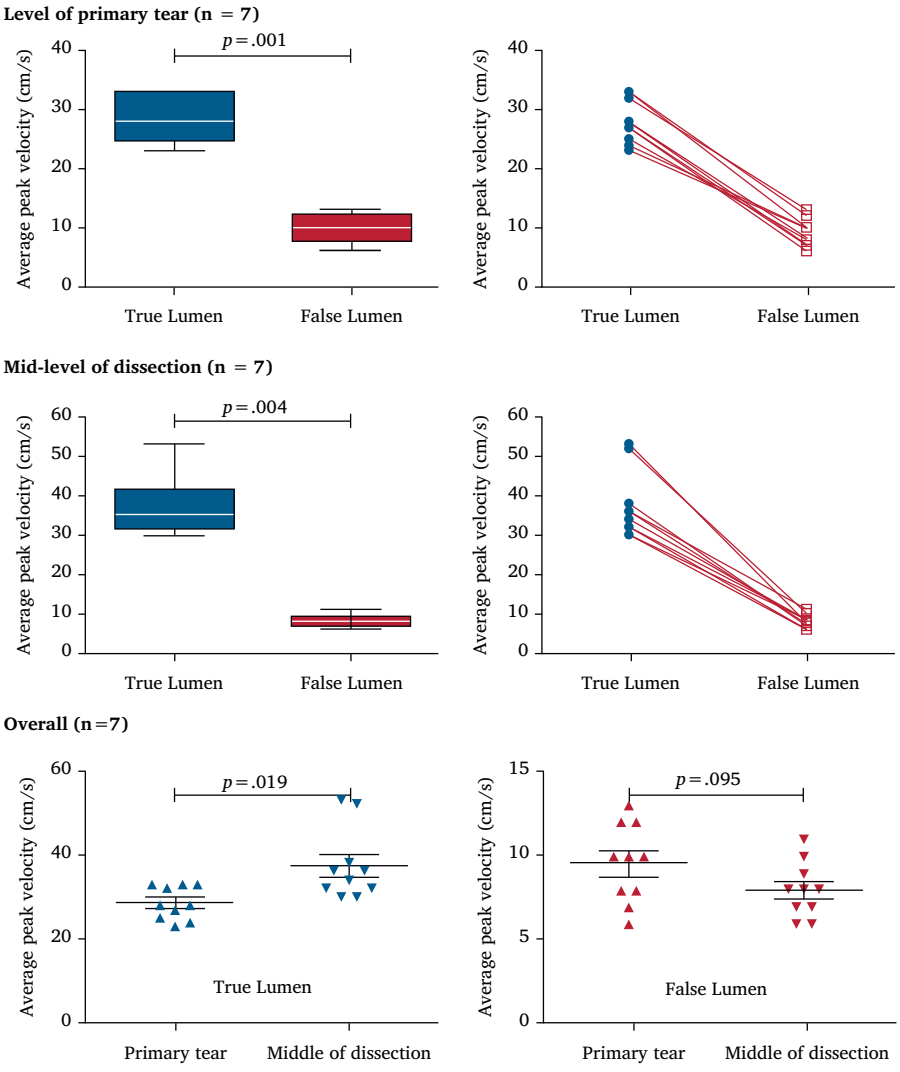

Figure 4. Box and whisker and line plots of the average peak velocity (APV) measured by Doppler wires in the true and false lumen in 7 animals. The box plots provide a graphical description of the differences between the true and false lumens, whereas the individual line plots show paired observations for each swine in the type B aortic dissection models and demonstrate the variations between swine. The median APV is greater in the true than in the false lumen at the levels of the primary tear and the middle of the dissection. The APV shows an apparent increase from the primary tear to the middle of dissection based on overall observations of the true lumen. However, the APV in the false lumen does not differ significantly between the two segments.

subsequent dissection propagation, especially in animal with deep intimal tears. A similar finding was reported by Mitsui et al.,[22] who suggested that the development of a dissection depends upon whether the intimal tear reaches the first third of the external media. This previous *in vitro* study using canine aortas demonstrated that a dissection progressed more often (85.7% of the time) when the intimal tear was located in the first third of the external media than when it was in any other layer. Additionally, van Baardwijk et al. reported an association between a deeper intimal tear and a slower dissection rate,[23] and suggested that the depth of the intimal tear probably determined whether a dissection extended into a branch or ripped around the base of the branch. There may be some reasons for this completely contrary finding of van Baardwijk et al.[23] First, their *ex vivo* experiments of aortic dissection in canine thoracic aorta were carried out in 1978, using a simple pulsatile pressure system with no flow, which might lead to an approximate result. Second, the dissection rate was only observed during the limited period of experiment instead of the process of propagation over time in an *in vivo* environment, giving a misplaced impression of dissection propagation.

Studies on the pathogenesis of dissection are viewed as clinically important in risk stratification because any further progression of the dissection may cause rupture by tearing to the adventitial side or may cause re-entry by tearing to the intimal side.[1,24] However, the question of how the

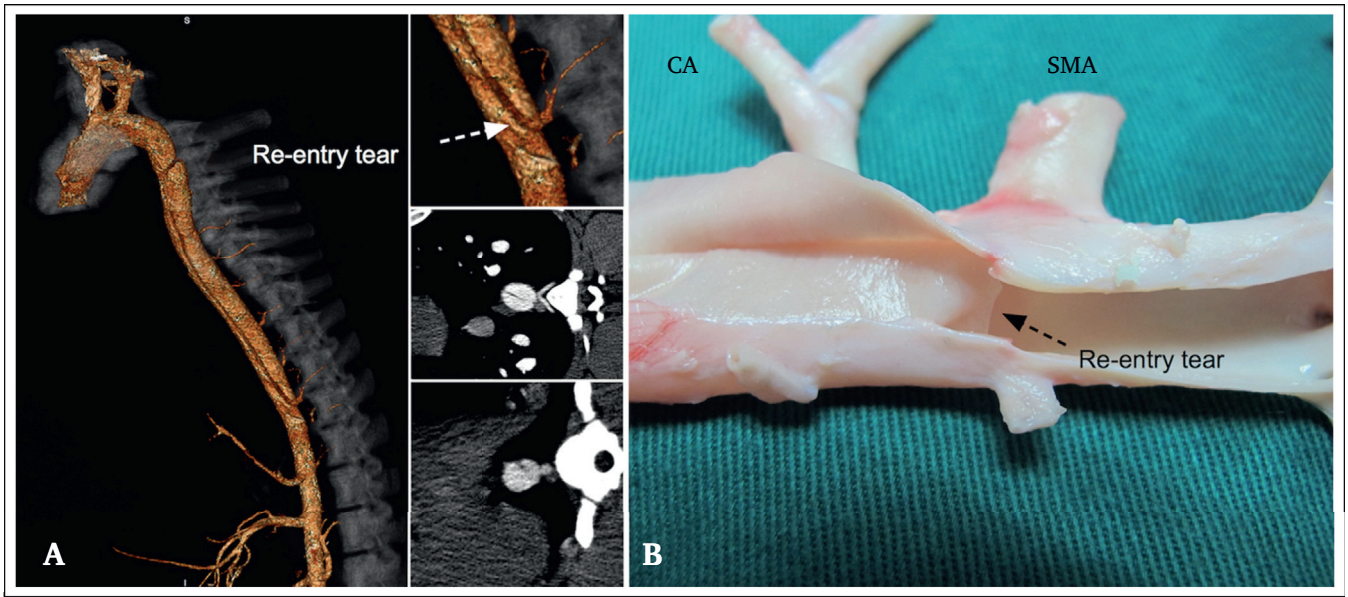

Figure 5. (A) In model A, the computed tomography (CT) imaging of one animal during follow up showed a re-entry tear located just at the ostium of an intercostal artery. (B) In model B, a flap tear occurred back to the aortic lumen around the base of the superior mesenteric artery (SMA). CA = coeliac artery.

dissecting layer influences the dissection propagation remains unanswered.

Interestingly, dissections can propagate either toward the internal elastic membrane or toward the external elastic membrane during peeling in the axial direction.[25] The histological findings in the present study indicated that the fibres on the adventitia and outside the media were much more stretched than those inside the media in both models, which suggested that the outside collagen fibres of the FL would reach their straightened lengths and that the adventitia would change to a stiff "jacket like" tube that would prevent arterial overstretching and rupture. van Baardwijk et al. observed that some layers of elastin in sheep aorto-intercostal junctions extended continuously from the aorta into the intercostal media,[26] whereas other aortic elastin was joined to the internal elastic lamina. Therefore, if the dissecting layer remains toward the external media, the dissection will extend into the branch media and potentially cause branch malperfusion. If the dissecting layer remains more toward the intimal side, then the dissection might extend around the branch site or re-enter the aortic lumen around the base of the branch. In the present study, the re-entry tears were found superficial and most frequently (80%) at the ostia of the aortic branch vessels in both models, which may be related to the biomechanics of dissection propagation. The superficial re-entry tears in both models also suggested that the dissecting layers would re-enter the aortic lumen. Faure et al. visually confirmed the finding that the abdominal aortic side branches, as the preferred location for re-entry tears, are anatomical barriers against distal and aneurysmal expansion of a dissection.[27]

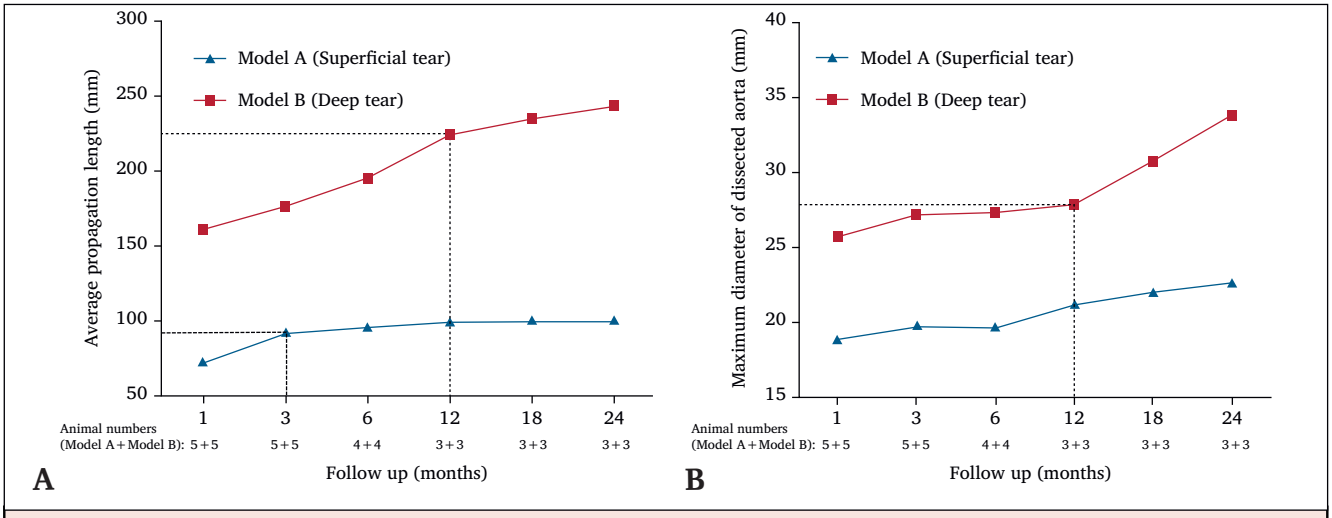

Figure 6. The trends of (A) average propagation length and (B) maximum diameter of dissection between the two models over time.

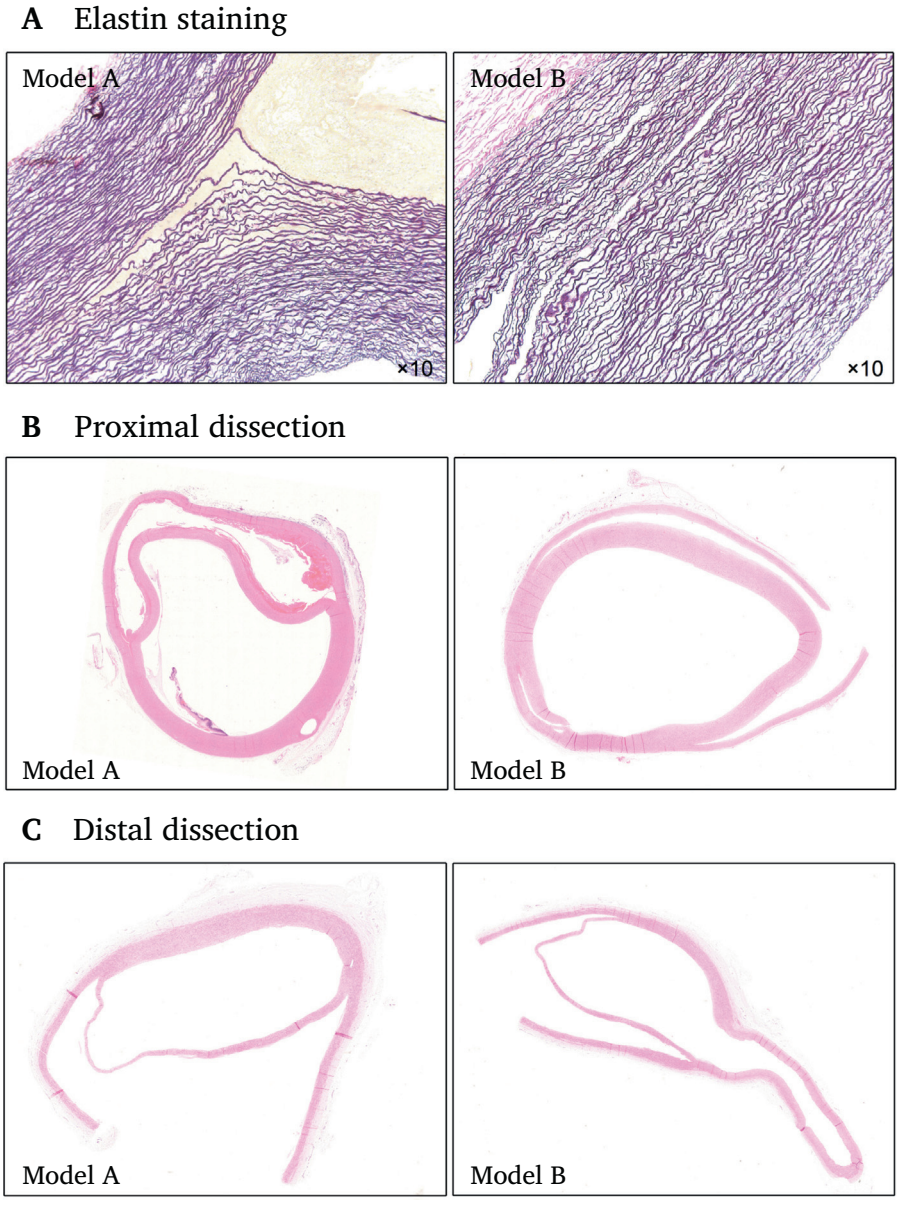

Figure 7. (A) Microscopy examination of elastin staining (resorcinol alkaline fuchsin stain, magnification × 10) showing the destruction of elastic lamellar architecture in the media layer of aortic wall. In both models, the elastic fibres were much more stretched on the adventitial side of false lumen than those on the intimal side. (B) In the proximal dissection (hematoxylin and eosin staining), the intimal tear of model B was identified to be deeper than that of model A. (C) However, the intimal tears in both groups developed to be superficial and similar in the distal dissection.

Factors that influence the TBAD haemodynamic distribution (pre-thoracic endovascular aneurysm repair [TEVAR]) and redistribution (post-TEVAR) were identified to be the key indicators of late adverse events.[28] For example, the intimal flap separates the TL and FL and its movement balances the blood pressures in the channels during cardiac cycles and during the transition from the acute to the chronic stage. Peterss et al. demonstrated an association between elastin fragmentation and subsequent increased fibrosis with imaging findings of thickened dissection flaps that showed loss of mobility.[29] The presented models were created by the same experienced vascular surgeons and established the protocol after a period of exploration and training. A thin or a thick intimal flap was created with the same pockets and circumferential cuts. Intra-operatively, a notably greater dissection propagation length was observed in animals with thick intimal flaps (model B), suggesting that different intimal shear stress and aortic wall strength caused by different aortic wall layers may play a major role in the acute propagation of dissection. The findings also demonstrated that the acute dissection propagation occurred any time but was most common in the first three months in model A and in the first 12 months in model B. Notably, the diameter of the aortic dissection seemed to

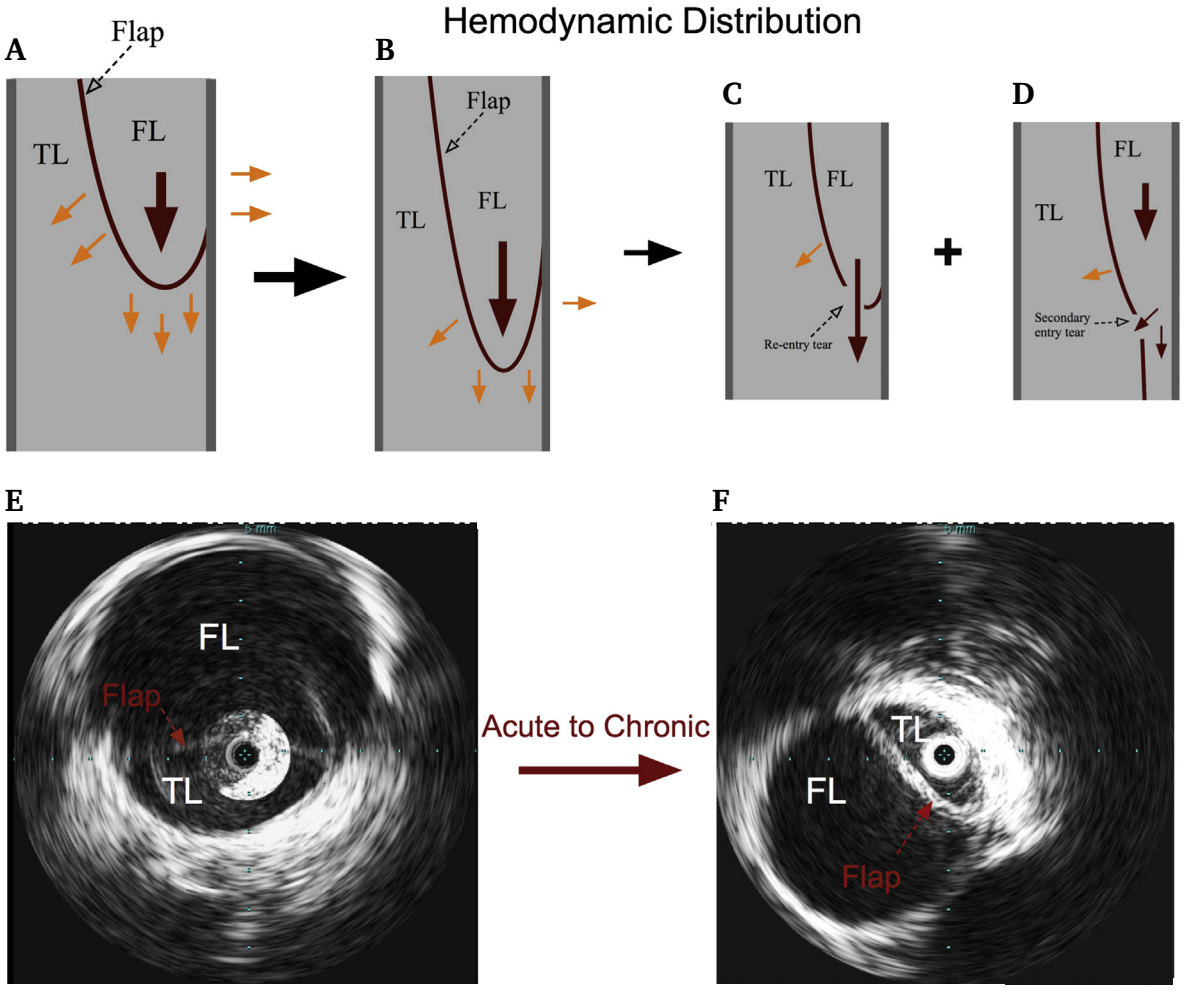

Figure 8. Diagram of the hemodynamic distribution and dynamic flap motion in aortic dissection. (A and B) Flow distribution in an acute dissection propagation demonstrated that the movement of the flap, inflow, outflow, primary tearing, and re-entry tearing contributed to maintaining the stability of the dissection hemodynamics. (C and D) At the subacute stage of dissection, the antegrade or retrograde blood flow across the secondary tears also kept a relatively balanced pressure gradient between the TL and FL. (E) Intravascular ultrasound imaging revealed that the intimal flap was thin at the acute phase, indicating large-scale motion over the course of the cardiac cycle. (F) However, the flap thickened and straightened over time, resulting in reduced motion. TL, true lumen; FL, false lumen.

grow faster when the dissection propagated slowly. In the acute and subacute stages, an increase in inflow and low or no outflow would increase the FL pressure, which would cause the TL to collapse or trigger acute propagation.[30] In the chronic stage, both the increased diameter and thrombosis in the FL may be other factors helping to keep this balance. No thrombosis formed in the FLs perhaps related to the antiplatelet therapy and the continuous inflow and outflow through the tears.

In the present study, the haemodynamic measurements using Doppler wires were deemed feasible and valuable for understanding the flow velocity distribution in the TL and FL. The findings suggested that although inflow increased in the FL, the average peak velocity was significantly lower than that in the TL. At the early stage of dissection, a high resistance existed in the FL, as no re-entry tear developed. Consequently, the flow velocity remained much lower in the FL, despite the increased volume and inflow into the FL. Notably, one prominent limitation for Doppler wire measurements is the lack of details available in a cycle. Peelukhana et al. suggested that during the systolic phase, the flap curved towards the FL and caused a complete obstruction of the TL.[31] Flow distribution in TBAD is influenced by the primary tear, the flap, the flow resistance, and the morphology of the TL and FL (Fig. 8).

The present study had some limitations. It used only a limited number of animals in each TBAD model, even though both were confirmed as repeatable models and achieved promising results. The models were also created using healthy swine, which had no intrinsic aortic disease; however, dissections in humans mostly occur in cases of hypertension, atherosclerosis, or degenerative changes in the media. Dissection propagation in the swine models may differ therefore from dissections in human patients. This was also the first attempt to use Doppler FloWires for aortic

dissection measurements, so only the present experience can be drawn upon (Appendix S1).

CONCLUSION

In this swine model of TBAD, the depth of the intimal tear had a significant direct relationship with aortic dissection propagation, especially in the model with a deep tear. The *in vivo* TBAD model may provide a valuable insight into the research onhaemodynamics and propagation in human aortic dissection.

CONFLICTS OF INTEREST

None.

FUNDING

This research is financially supported by the National Natural Science Foundation of China (81470573, 81770474, 81371648, 81770508), and is also sponsored by the Shanghai Sailing Program (No.18YF1404000), and Shanghai Committee of Science and Technology, China (No.16410722900).

ACKNOWLEDGMENTS

The authors would like to thank professor Nigel Wood (Chemical Engineering Imperial College London) for his support of aortic haemodynamics. The authors also thank David Shong Un Wong (Philips IGT-Devices) for his excellent technical assistance in Doppler measurements.

APPENDIX A. SUPPLEMENTARY DATA

Supplementary data to this article can be found online at https://doi.org/10.1016/j.ejvs.2019.02.026.

REFERENCES

1 Nienaber CA, Clough RE. Management of acute aortic dissection. *Lancet* 2015;**385**:800–11.
2 Tsamis A, Krawiec JT, Vorp DA. Elastin and collagen fibre microstructure of the human aorta in ageing and disease: a review. *J R Soc Interface* 2013;**10**:20121004.
3 Veger HT, Westenberg JJ, Visser MJ. The role of branch vessels in aortic type B dissection: an *in vitro* study. *Eur J Vasc Endovasc Surg* 2015;**49**:375–81.
4 Yu SC, Liu W, Wong RH, Underwood M, Wang D. The potential of computational fluid dynamics simulation on serial monitoring of hemodynamic change in type B aortic dissection. *Cardiovasc Intervent Radiol* 2016;**39**:1090–8.
5 Ben Ahmed S, Dillon-Murphy D, Figueroa CA. Computational study of anatomical risk factors in idealized models of type B aortic dissection. *Eur J Vasc Endovasc Surg* 2016;**52**:736–45.
6 Cheng Z, Riga C, Chan J, Hamady M, Wood NB, Cheshire NJ, et al. Initial findings and potential applicability of computational simulation of the aorta in acute type B dissection. *J Vasc Surg* 2013;**57**:35S–43S.
7 Beller CJ, Labrosse MR, Thubrikar MJ, Robicsek F. Finite element modeling of the thoracic aorta: including aortic root motion to evaluate the risk of aortic dissection. *J Med Eng Technol* 2008;**32**:167–70.
8 Nathan DP, Xu C, Gorman 3rd JH, Fairman RM, Bavaria JE, Gorman RC, et al. Pathogenesis of acute aortic dissection: a finite element stress analysis. *Ann Thorac Surg* 2011;**91**:458–63.
9 Chen HY, Peelukhana SV, Berwick ZC, Kratzberg J, Krieger JF, Roeder B, et al. Fluid–structure interaction simulations of aortic dissection with bench validation. *Eur J Vasc Endovasc Surg* 2016;**52**:589–95.
10 Alimohammadi M, Sherwood JM, Karimpour M, Agu O, Balabani S, Diaz-Zuccarini V. Aortic dissection simulation models for clinical support: fluid–structure interaction vs. rigid wall models. *Biomed Eng Online* 2015;**14**:34.
11 Williams DM, Lee DY, Hamilton BH, Marx MV, Narasimham DL, Kazanjian SN, et al. The dissected aorta: percutaneous treatment of ischemic complications: principles and results. *J Vasc Interv Radiol* 1997;**8**:605–25.
12 Chung JW, Elkins C, Sakai T, Kato N, Vestring T, Semba CP, et al. True-lumen collapse in aortic dissection: part I. Evaluation of causative factors in phantoms with pulsatile flow. *Radiology* 2000;**214**:87–98.
13 Riambau V, Bockler D, Brunkwall J, Cao P, Chiesa R, Coppi G, et al. Editor's Choice - management of descending thoracic aorta diseases: clinical Practice guidelines of the European Society for vascular Surgery (ESVS). *Eur J Vasc Endovasc Surg* 2017;**53**:4–52.
14 Erbel R, Aboyans V, Boileau C, Bossone E, Bartolomeo RD, Eggebrecht H, et al. ESC Committee for Practice Guidelines. 2014 ESC guidelines on the diagnosis and treatment of aortic diseases: document covering acute and chronic aortic diseases of the thoracic and abdominal aorta of the adult. The Task Force for the diagnosis and treatment of aortic diseases of the European Society of Cardiology (ESC). *Eur Heart J* 2014;**35**:2873–926.
15 Terai H, Tamura N, Yuasa S, Nakamura T, Shimizu Y, Komeda M. An experimental model of Stanford type B aortic dissection. *J Vasc Interv Radiol* 2005;**16**:515–9.
16 Cui JS, Zhuang SJ, Zhang J, Mei ZJ, Jing ZP, Liao MF. Two-end intimal flap suturing method for establishing Stanford type B aortic dissection in a canine model. *Eur J Vasc Endovasc Surg* 2009;**38**:603–7.
17 Tang J, Wang Y, Hang W, Fu W, Jing Z. Controllable and uncontrollable Stanford type B aortic dissection in canine models. *Eur Surg Res* 2010;**44**:179–84.
18 Razavi MK, Nishimura E, Slonim S, Zeigler W, Kee S, Witherall HL, et al. Percutaneous creation of acute type-B aortic dissection: an experimental model for endoluminal therapy. *J Vasc Interv Radiol* 1998;**9**:626–32.
19 Okuno T, Yamaguchi M, Okada T, Takahashi T, Sakamoto N, Ueshima E, et al. Endovascular creation of aortic dissection in a swine model with technical considerations. *J Vasc Surg* 2012;**55**:1410–8.
20 de Beaufort HWL, Ferrara A, Conti M, Moll FL, van Herwaarden JA, Figueroa CA, et al. Comparative analysis of porcine and human thoracic aortic stiffness. *Eur J Vasc Endovasc Surg* 2018;**55**:560–6.
21 Qing KX, Chan YC, Lau SF, Yiu WK, Ting AC, Cheng SW. *Ex vivo* haemodynamic models for the study of Stanford type B aortic dissection in isolated porcine aorta. *Eur J Vasc Endovasc Surg* 2012;**44**:399–405.
22 Mitsui H, Uchida H, Teramoto S. Correlation between the layer of an intimal tear and the progression of aortic dissection. *Acta Med Okayama* 1994;**48**:93–9.
23 van Baardwijk C, Roach MR. Factors in the propagation of aortic dissections in canine thoracic aortas. *J Biomech* 1987;**20**:67–73.
24 Khoynezhad A, White RA. Pathogenesis and management of retrograde type A aortic dissection after thoracic endovascular aortic repair. *Ann Vasc Surg* 2013;**27**:1201–6.
25 Sommer G, Gasser TC, Regitnig P, Auer M, Holzapfel GA. Dissection properties of the human aortic media: an experimental study. *J Biomech Eng* 2008;**130**:021007.
26 van Baardwijk C, Barwick SE, Roach MR. Organization of medial elastin at aortic junctions in sheep and lambs. *Can J Physiol Pharmacol* 1985;**63**:855–62.

27 Faure EM, Canaud L, Cathala P, Serres I, Marty-Ane C, Alric P. Human ex vivo model of Stanford type B aortic dissection. *J Vasc Surg* 2014;**60**:767–75.
28 Menichini C, Pirola S, Guo B, Fu W, Dong Z, Xu XY. High wall stress may predict the formation of stent-graft-induced new entries after thoracic endovascular aortic repair. *J Endovasc Ther* 2018;**25**:571–7.
29 Peterss S, Mansour AM, Ross JA, Vaitkeviciute I, Charilaou P, Dumfarth J, et al. Changing pathology of the thoracic aorta from acute to chronic dissection: literature review and insights. *J Am Coll Cardiol* 2016;**68**:1054–65.
30 Chung JW, Elkins C, Sakai T, Kato N, Vestring T, Semba CP, et al. True-lumen collapse in aortic dissection: part II. Evaluation of treatment methods in phantoms with pulsatile flow. *Radiology* 2000;**214**:99–106.
31 Peelukhana SV, Wang Y, Berwick Z, Kratzberg J, Krieger J, Roeder B, et al. Role of pulse pressure and geometry of primary entry tear in acute type B dissection propagation. *Ann Biomed Eng* 2017;**45**:592–603.

Eur J Vasc Endovasc Surg (2019) 58, 425

COUP D'OEIL

Rare Presentation of a Retroperitoneal Tumour in a Young Male

Chrysanthi P. Papageorgopoulou *, **Konstantinos M. Nikolakopoulos**
Department of Vascular Surgery, University Hospital of Patras, Patras, Greece

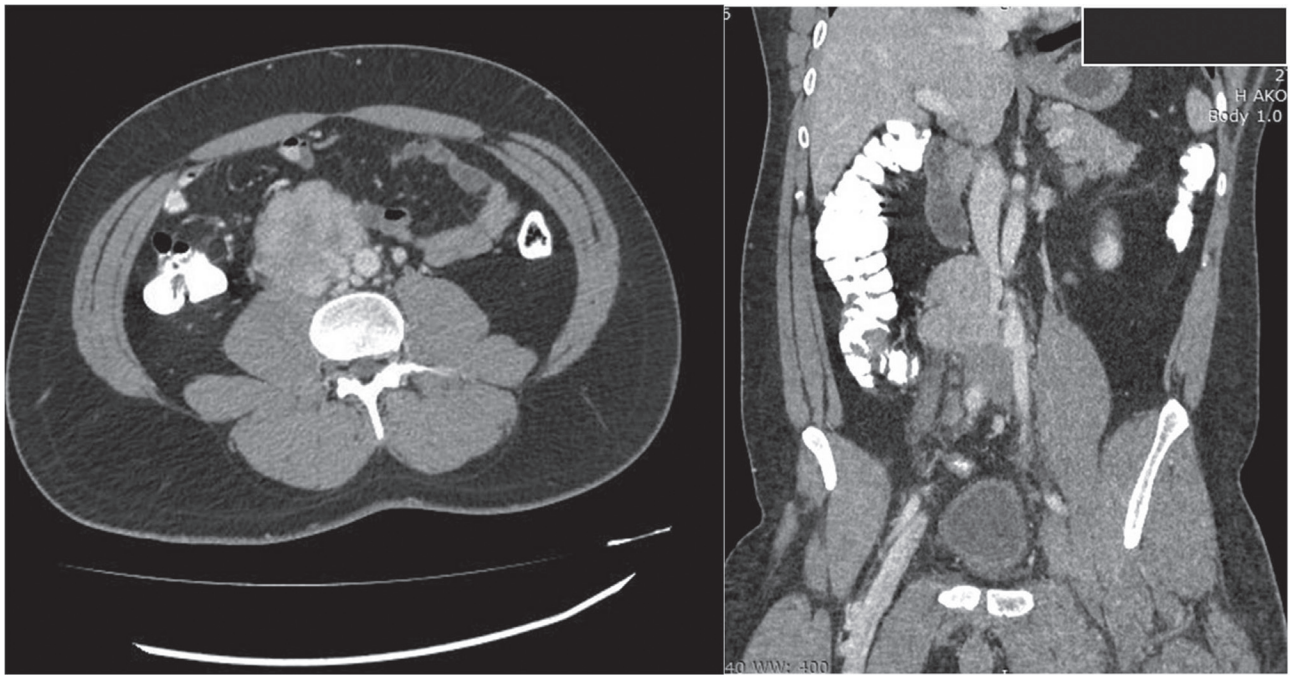

A 33 year old man presented to the emergency department with a seven day history of the right lower extremity oedema. Physical examination revealed calf and thigh oedema, tenderness, and erythema. Duplex ultrasound scanning failed to diagnose any deep venous obstruction but a computed tomography (CT) venogram revealed a retroperitoneal mass compressing the inferior vena cava (Fig. 1). This was biopsied under CT guidance and a grade 1 leiomyosarcoma was diagnosed. After three months of treatment with low molecular weight heparin and neoadjuvant therapy, the oedema was reduced and the sarcoma was resected successfully.

* Corresponding author. Department of Vascular Surgery, University Hospital of Patras, Patras, Greece.
E-mail address: chrisanthi.papageorg@gmail.com (Chrysanthi P. Papageorgopoulou).

https://doi.org/10.1016/j.ejvs.2019.05.005